Single-Mode Propagation of Mutual Temporal Coherence: Equivalence of Time and Frequency Measurements of Polarization Mode Dispersion

Brian Heffner
Instruments and Photonics Laboratory
HPL-94-22
March, 1994

optical, fiber optics, photonic subsystems, incoherent, photonics, lightwave components

A formalism is presented for treatment of the mutual temporal coherence between orthogonal polarization modes in single-mode optical systems, permitting calculation of the effect of propagation through birefringent devices upon this coherence. We demonstrate that, allowing for differences similar to the birefringent effects of fiber pigtails, polarization mode dispersion data measured using frequency-scanning techniques are related by the Fourier transform to data measured using interferometric techniques.

Even in single-mode fiber and in components where optical propagation is restricted to a single spatial mode, it is possible for two polarization modes to propagate, each according to its own phase delay and group delay. Polarization mode dispersion (PMD) is a term used to describe the effect of propagation through a device in which the two group delays are unequal. Owing to the unequal group delays, propagation through such a device will change the mutual temporal coherence between the two polarization modes. Likewise, the two unequal phase delays lead to a frequency-dependent output state of polarization (SOP) in response to a fixed input SOP.

Measurement of the differential group delay (DGD) is important to the characterization of optical fibers and components because it determines the severity of the deleterious effects of PMD. These effects include pulse distortion which may limit transmission bandwidths of high-speed digital links, and interactions with laser chirp and polarization-dependent loss which may lead to nonlinear behavior in analog links. Among the techniques widely used to measure DGD, an interferometric technique [1,2] measures the effect of PMD upon mutual coherence, and a frequency-scanning technique [3] measures the effect of PMD, through variations of the output SOP, upon transmission through a fixed analyzer.

In this letter a formalism is introduced which permits calculation of the propagation of mutual coherence through a single-mode device. We show that the data measured using the frequency-scanning technique is related by the Fourier transform to data measured using the interferometric technique, so that either data set can be used to calculate an approximation of the other. This relationship is confirmed experimentally. We also explain why the two data sets are not rigorously linked by the Wiener-Khinchin relation between correlations and spectral densities. The results of this letter apply generally to all linear, time-invariant (LTI) devices, and do not depend upon assumptions of extensive polarization mode coupling.

As originally introduced, the elements of the Jones vector $\boldsymbol{a}$ represented the x and y components of the electric field vector of the propagating light wave at a fixed point in space [4]. All fields were assumed to be periodic, and since only LTI devices were treated the ubiquitous periodic phase term $\exp(i2\pi\nu t)$ could be dropped. The remaining amplitude and phase terms formed a vector which described the optical polarization.

The usefulness of the Jones calculus can be significantly broadened by dealing with vectors and matrices which are functions of the optical frequency ν. This allows treatment of nonperiodic signals, as the frequency-dependent electric field vector $\boldsymbol{a}(\nu)$ can be related to the time-dependent electric field vector $\underline{\boldsymbol{a}}(t)$ through the Fourier transform: $\underline{\boldsymbol{a}}(t) \supset \boldsymbol{a}(\nu)$. (The symbol $\supset$ is used to denote both forward and inverse Fourier transform relations: $\underline{\boldsymbol{a}}(t) = \int \boldsymbol{a}(\nu) \exp(-i2\pi\nu t)\, d\nu$ and $\boldsymbol{a}(\nu) = \int \underline{\boldsymbol{a}}(t) \exp(i2\pi\nu t)\, dt$.) When $\boldsymbol{a}(\nu)$ is zero for negative frequencies, each component of $\underline{\boldsymbol{a}}(t)$ is an analytic signal associated with the real electric field. Any LTI device can be characterized by an impulse response matrix $\underline{\boldsymbol{T}}(t)$ as well as by a frequency response matrix $\boldsymbol{T}(\nu)$, the two matrices again forming a Fourier transform pair: $\underline{\boldsymbol{T}}(t) \supset \boldsymbol{T}(\nu)$. The relationship between the input field $\boldsymbol{a}(\nu)$ and the output field $\boldsymbol{b}(\nu)$ is then represented by multiplication in the frequency domain, and is equivalently represented by convolution in the time domain, i.e. $\underline{\boldsymbol{b}}(t) = \underline{\boldsymbol{T}}(t) * \underline{\boldsymbol{a}}(t) \quad \supset \quad \boldsymbol{b}(\nu) = \boldsymbol{T}(\nu)\, \boldsymbol{a}(\nu)$, where the matrix convolution is carried out similarly to matrix multiplication.

In describing the evolution of temporal coherence, the following *mutual coherence matrix* will be shown to be very useful:

$$\underline{\boldsymbol{G}}_a(\tau) \equiv \langle \underline{\boldsymbol{a}}(t+\tau)\, \underline{\boldsymbol{a}}^{\dagger}(t) \rangle = \begin{bmatrix} \langle \underline{a}_x(t+\tau)\, \underline{a}_x^*(t) \rangle & \langle \underline{a}_x(t+\tau)\, \underline{a}_y^*(t) \rangle \\ \langle \underline{a}_y(t+\tau)\, \underline{a}_x^*(t) \rangle & \langle \underline{a}_y(t+\tau)\, \underline{a}_y^*(t) \rangle \end{bmatrix} \tag{1}$$

The superscript * indicates complex conjugation, $\underline{\boldsymbol{a}}^{\dagger}$ is the transposed complex conjugate of $\underline{\boldsymbol{a}}$, and angled brackets indicate a time average as defined in Eq. (3). From this definition we see that the diagonal elements of $\underline{\boldsymbol{G}}_a(\tau)$ are the self coherence functions of the x and y polarizations, that the antidiagonal elements of $\underline{\boldsymbol{G}}_a(\tau)$ are the mutual coherence functions of the x and y polarizations, and that $\underline{\boldsymbol{G}}_a(0)$ is the coherency matrix [5]. The Fourier transforms of these coherence functions have been shown [5] to be the spectral densities $G_{a,\,xx}(\nu)$ and $G_{a,\,yy}(\nu)$, and the mutual spectral densities $G_{a,\,xy}(\nu)$ and $G_{a,\,yx}(\nu)$, respectively. These spectral densities define the elements of the *mutual spectral density matrix* $\boldsymbol{G}_a(\nu)$:

$$\underline{\boldsymbol{G}}_a(\tau) \quad \supset \quad \boldsymbol{G}_a(\nu) = \begin{bmatrix} G_{a,\,xx}(\nu) & G_{a,\,xy}(\nu) \\ G_{a,\,yx}(\nu) & G_{a,\,yy}(\nu) \end{bmatrix} \tag{2}$$

Given the mutual coherence matrix $\underline{\boldsymbol{G}}_a(\tau)$ at the input to a LTI device whose impulse response is $\underline{\boldsymbol{T}}(t)$, it is possible to calculate the mutual coherence matrix at the output

$\underline{G}_b(\tau)$ by expanding the definition of $\underline{G}_b(\tau)$ in terms of the input-output relation $\underline{b}(t) = \underline{T}(t) * \underline{a}(t)$:

$$\begin{aligned}\underline{G}_b(\tau) &\equiv \lim_{T\to\infty} \frac{1}{2T}\int_{-T}^{T} \underline{b}(t+\tau)\,\underline{b}^\dagger(t)\,dt \\ &= \lim_{T\to\infty} \frac{1}{2T}\int_{-T}^{T} \int_{-\infty}^{\infty} \underline{T}(t+\tau-u)\,\underline{a}(u)\,du \int_{-\infty}^{\infty} \underline{a}^\dagger(w)\,\underline{T}^\dagger(t-w)\,dw\,dt \end{aligned} \tag{3}$$

When the processes $\underline{a}_x(t)$ and $\underline{a}_y(t)$ are jointly wide-sense stationary, Eq. (3) can be compactly expressed in both the time and frequency domains:

$$\underline{G}_b(\tau) = \underline{T}(\tau) * \underline{G}_a(\tau) * \underline{T}^\dagger(-\tau) \quad \supset \quad G_b(\nu) = T(\nu)\; G_a(\nu)\; T^\dagger(\nu) \tag{4}$$

Two techniques widely used for PMD measurement, frequency scanning and interferometry, are illustrated schematically in Fig. 1. For interferometric measurements the shutter is left open and the scanning monochromator is removed from the measurement system. Collimated light from a broadband light emitting diode is polarized and split into two mutually coherent beams. One mirror can be scanned in position, creating a differential delay of $\varepsilon = 2d/c$ between the two orthogonal polarizations which are recombined and directed through the DUT. When photocurrent is measured as a function of ε, coherent fringes can be observed only when this differential delay is compensated by the DGD of the DUT. For frequency scanning measurements the shutter is closed, and the scanning monochromator is included in the measurement system so that the photocurrent is proportional to spectral density. With the shutter closed, the mirrors and beamsplitter are superfluous and the entire apparatus left of the DUT can effectively be replaced by an LED followed by a polarizer. PMD in the DUT leads to ripples in the measured spectral density, and the DGD is proportional to the number of extrema in a given frequency span. Details of interpretation of both measurements can be found in references [1, 2 and 3].

The measured results of each technique are related to Eq. (4) as follows. The interferometric technique measures photocurrent I as a function of differential delay ε, and the horizontal polarizer ahead of the photodiode causes $I(\varepsilon)$ to be given by the xx component of $r\,\underline{G}_b(\tau)$ evaluated at $\tau = 0$, where r is the effective responsivity of the photodiode. The frequency scanning technique measures photocurrent as a function of optical frequency, and the horizontal polarizer ahead of the scanning monochromator causes $I(\nu)$ to be given by the xx component of $r\,G_b(\nu)$. If the polarized LED signal is represented by the self coherence function $\underline{u}(\tau)$ and the spectral density $u(\nu)$, we can express the mutual coherence matrix appropriate for the interferometric calculation and the mutual spectral density matrix appropriate for the frequency scanning calculation, respectively, as

$$\underline{\boldsymbol{G}}_a(\tau) = \begin{bmatrix} \underline{u}(\tau) & \underline{u}(\tau-\varepsilon) \\ \underline{u}(\tau+\varepsilon) & \underline{u}(\tau) \end{bmatrix} \quad \text{and} \quad \boldsymbol{G}'_a(\nu) = \begin{bmatrix} u(\nu) & 0 \\ 0 & 0 \end{bmatrix}. \tag{5}$$

The two expressions above do *not* form a Fourier transform pair because the shutter of Fig. 1 is open for the interferometric measurement and closed for the frequency scanning measurement. Consequently, the data measured using the two techniques are not directly related by the Wiener-Khinchin theorem.

A simple example will illustrate these relationships. Suppose the DUT of Fig. 1 comprises a waveplate of retardance $\lambda/2$ and orientation θ, which models the birefringence of a fiber pigtail, followed by a birefringent crystal exhibiting a frequency-independent DGD of 2γ whose eigenmodes are linear SOPs oriented at $\pm 45°$. The Jones matrix [6] and impulse response of this DUT can be shown to be

$$\boldsymbol{T}(\nu) = \begin{bmatrix} cC + isS & sC - icS \\ sC + icS & -cC + isS \end{bmatrix} \subset \underline{\boldsymbol{T}}(t) = \frac{1}{2}\begin{bmatrix} \alpha\delta^+ - \beta\delta^- & \beta\delta^+ + \alpha\delta^- \\ \alpha\delta^+ + \beta\delta^- & \beta\delta^+ - \alpha\delta^- \end{bmatrix}, \tag{6}$$

where $c = \cos 2\theta$, $s = \sin 2\theta$, $C = \cos 2\pi\nu\gamma$, $S = \sin 2\pi\nu\gamma$, $\alpha = s + c$, $\beta = s - c$, and we use the Dirac delta functions $\delta^+ = \delta(t+\gamma)$ and $\delta^- = \delta(t-\gamma)$. Application of Eq. (4) yields the measurable photocurrent for each technique:

$$I(\varepsilon) = r\underline{\boldsymbol{G}}_{b,xx}\Big|_{\tau=0} = \frac{r}{2}[2\underline{u}(0) + (1+\sin 4\theta)\,\underline{u}(\varepsilon - 2\gamma) - (1 - \sin 4\theta)\,\underline{u}(\varepsilon + 2\gamma)] \tag{7}$$

$$I(\nu) = r\boldsymbol{G}'_{b,xx}(\nu) = \frac{r}{2}[1 + \cos 4\theta \cos 4\pi\nu\gamma]\,u(\nu) \tag{8}$$

Although the two photocurrents above do not constitute a Fourier transform pair, let us examine their differences from an exact transform pair in light of the relation $[1 + 2\cos 4\pi\nu\gamma]\,u(\nu) \subset \underline{u}(\varepsilon) + \underline{u}(\varepsilon - 2\gamma) + \underline{u}(\varepsilon + 2\gamma)$. Two differences from an exact transform pair are apparent: Constant terms may be lost, and the relative amplitudes of the fringe patterns centered at different relative delays may vary in response to changes in the pigtail birefringence between the measurement system and the input to the DUT, although the relative delays will not be affected. Changes in the pigtail birefringence between the measurement system and the output of the DUT have a similar effect.

In order to show experimentally the approximate Fourier transform relationship between $I(\nu)$ measured using the frequency-scanning technique and $I(\varepsilon)$ measured using the interferometric technique, the data measured by each technique are compared to the Fourier-transformed data measured by the other technique. Two DUTs were measured. The first DUT comprised two sections of birefringent fiber which were spliced together with a deliberate angular misalignment, providing a single site for polarization mode coupling. The second DUT was a 6-km length of single-mode fiber wound on a 30-cm diameter spool, allowing for continuous mode coupling over the length of the fiber. For each DUT, interferometric data were measured as a function of relative delay using the apparatus of Fig. 1 with the shutter open and the scanning monochromator removed. Frequency scanning data were then measured as a function of optical frequency after closing the shutter and inserting the scanning monochromator. Directly measured data are shown in traces A, B, E and F of Fig. 2. Two even spectral density functions were formed from traces B and F by replicating the positive-frequency components at negative frequencies. These two even functions generated traces C and G through an inverse discrete Fourier transform algorithm. Two even mutual coherence functions were then formed from traces A and E by replacing the left-hand sides of those traces by reflections of their right-hand sides. These two even functions generated two spectral density functions through a discrete Fourier transform algorithm, and spectral densities at positive frequencies are shown in traces D and H. The spectrum of the LED was centered at approximately 229 THz, or 1309 nm.

The similarity of trace A to C and of trace E to G demonstrates that interferometric measurements can be approximated by transformed frequency scanning measurements. The placement of fringe patterns, indicating PMD, is similar in either case. Differences between traces A and C and between E and G are no greater than the changes measured as the fiber pigtails to the DUT are flexed to change their birefringences. Conversely, the similarity of trace B to D and of trace F to H demonstrates that frequency scanning measurements can be approximated by transformed interferometric measurements. The spectral density of extrema, indicating PMD, is similar in either case. Differences between traces B and D and between F and H are again no greater than the changes caused by pigtail effects.

In summary, a formalism has been presented which permits calculation of the effects of propagation through a general LTI birefringent device, with any degree of polarization mode coupling, upon the mutual temporal coherence between polarization modes. Interferometric measurement and frequency-scanning measurement of PMD have been shown to be related by the Fourier transform. Data measured using one technique can be Fourier transformed to approximate the data measured using the other technique.

The author thanks H. Lin of Hewlett-Packard Labs for the loan of measurement equipment.

References

[1] K. Mochizuki, Y. Namihira and H. Wakabayashi, Electron. Lett. **17**, 153 (1981).

[2] N. Gisin, J-P Von der Weid and J-P Pellaux, IEEE J. Lightwave Technol. **LT-9**, 821 (1991).

[3] C. D. Poole, Optics Lett. **14**, 523 (1989).

[4] R. C. Jones, J. Optical Soc. Am., **31**, 488 (1947).

[5] J. W. Goodman, *Statistical Optics*, (Wiley, New York, 1985).

[6] D. S. Kliger, J. W. Lewis and C. E. Randall, *Polarized Light in Optics and Spectroscopy*, (Academic, San Diego, 1990).

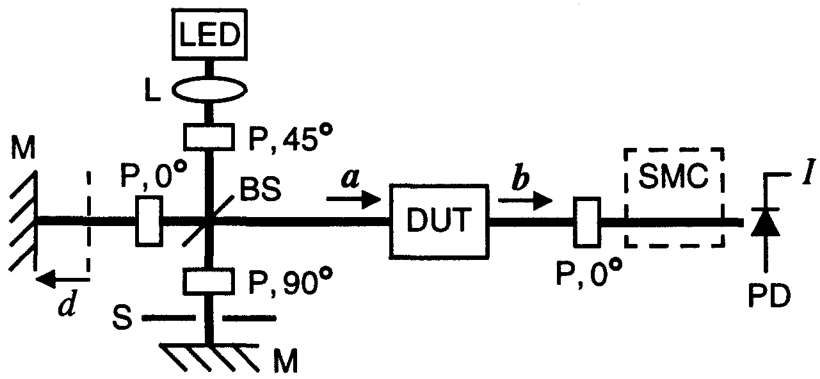

Figure 1. Apparatus used for measurement of polarization mode dispersion using frequency scanning and interferometry. LED: light emitting diode; L: lens; P: linear polarizer; BS: beamsplitter; M: mirror; DUT: device under test; SMC: scanning monochromator; PD: photodiode.

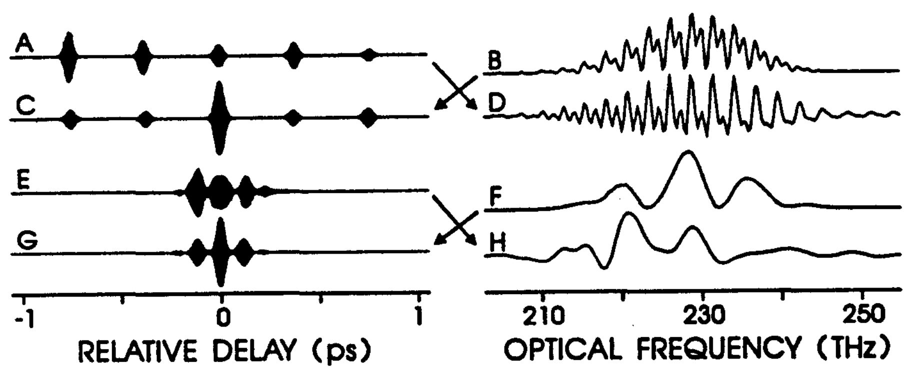

Figure 2. Photocurrents (linear scale) measured using the apparatus of Fig. 1. Interferometric (left) and frequency scanning (right) PMD measurements of a two-section birefringent fiber concatenation (A-D) and a 6-km spool of fiber (E-H). Traces A, B, E and F were measured directly. Traces C and G are inverse Fourier transforms of B and F. Traces D and H are Fourier transforms of the even functions formed by replacing the left-hand sides of traces A and E by reflections of their right-hand sides. Coherent fringes of the interferometric traces are spaced too densely to be visible at this scale.